Inertial Energy Distribution Error Control for Optimal Wind-Shear Penetration

K. Krishnakumar* and J. E. Bailey†
University of Alabama, Tuscaloosa, Alabama 35487

The principle of inertial energy distribution error control for optimal airplane microburst wind-shear penetration was developed, and a controller based on this principle was tested for its robustness in a realistic environment. A Monte Carlo approach together with a nonlinear simulation of a takeoff flight condition was used to evaluate system performance. Statistical models for the microburst strength, size, and location were used for the Monte Carlo simulation. A microburst-specific controller, based on a minimax height-loss performance index, was used in the Monte Carlo simulation as a reference controller. These trajectory results were compared with those of the controller based on an inertial energy distribution error performance index. The results obtained demonstrated two important concepts: 1) It is important to distribute inertial energy error equally between potential energy and inertial kinetic energy of the airplane system to minimize height losses. 2) Minimization of height loss results in maintaining an approximately constant inertial speed.

Nomenclature

E = total inertial energy, ft lb
$\dot{E}_{\text{airmass}}$ = total air mass relative energy rate, ft lb/s
E_d = inertial energy distribution, ft lb
E_{wind} = total energy component due to air mass motion, ft lb
H_A = height changes relative to the local air mass, ft
H_I = inertial height or inertial altitude, ft
H_{I0} = desired inertial altitude, ft
H_W = height associated with the vertical air mass motion, ft
h_{di} = specific inertial energy distribution error, ft
h_I = inertial height error in ft = $H_I - H_{I0}$
$J[u]$ = performance index
m = mass of the airplane, slugs
q = body-axis pitch rate, rad/s
T = thrust force, lb
U, W = body-axes velocities, ft/s
V_A = true airspeed, ft/s
V_I = total inertial velocity, ft/s
V_{I0} = desired total inertial velocity, ft/s
W_X = horizontal wind in earth axes, ft/s
W_Z = vertical wind in earth axes, ft/s
ΔW_X = horizontal wind shear
w_x, w_z = wind-axes components of atmospheric wind, ft/s
X_I = inertial position along X axis, ft
α = angle of attack, deg
γ_A = air mass relative flight-path angle; deg, rad
γ_I = absolute flight-path angle, deg, rad
δ_e = elevator deflection, rad, deg
δ_t = thrust coefficient (0–1)
θ = aircraft pitch angle, deg, rad
λ = energy distribution parameter
$(\dot{})$ = rate of change of ( )

Presented as Paper 89-0016 at the AIAA 27th Aerospace Sciences Meeting, Reno, NV, Jan. 9–12, 1989; received March 29, 1989; revision received July 31, 1989. Copyright © 1989 by K. Krishnakumar and J. E. Bailey. Published by the American Institute of Aeronautics and Astronautics, Inc., with permission.

*Assistant Professor, Department of Aerospace Engineering. Member AIAA.
†Professor, Department of Aerospace Engineering. Member AIAA.

Introduction

A MICROBURST is technically defined as a downburst of cool air that interacts with the Earth to cause, at low altitudes, a complex wind field that may have high wind shear and dilation. The hazardous nature of the microburst encounter during takeoff or landing is due to the airplane's loss of airspeed caused by the head wind shearing to tailwind and flight in the strong downdraft as the microburst is penetrated.[2] The loss of airspeed coupled with height loss from the downdraft may result in dangerous maneuvers at low altitudes during takeoff and landing phases of flight. Safe flight in a microburst environment depends on optimum energy management by the pilot or an autopilot. In this study, the basic principles of airplane energy management and energy control during the microburst encounter are emphasized. The principle of inertial energy distribution error control is developed theoretically, and a controller based on this principle is evaluated in a wide range of microburst environments using a nonlinear simulation of a transport aircraft.

An airplane flying through a microburst environment may have its energy states significantly modified or controlled. During a microburst penetration, the airplane loses energy (to the environment) by height and airspeed losses resulting from conservative and nonconservative transients. Understanding the energy flows in the airplane system, and the energy transfer from the airplane due to the microburst environment, can provide fundamental insight into the wind-shear encounter. Such an energy analysis was conducted by the authors in Ref. 1 and several energy-related performance measures for control system design were evaluated. (Figure 1 presents a comparison of the results obtained in Ref. 1 in terms of the maximum height loss encountered during a microburst encounter.) An energy performance measure based on inertial energy distribution was found in the earlier study[1] to yield the best control strategy for wind-shear encounters. Simply

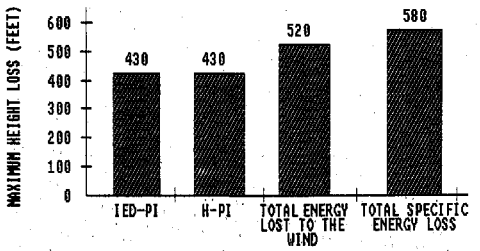

Fig. 1 Comparison of energy-related performance indices (from Ref. 1).

stated, this strategy suggests that the error in total airplane energy (either more energy due to increased engine thrust output or less energy due to the wind-shear encounter) should be equally distributed between the airplane potential energy and the airplane kinetic energy, in order to minimize deviations from the desired trajectory. This equidistribution of energy is realized by a feedback controller to yield minimum height-loss trajectories.

The lack of additional available energy (thrust limiting) during a typical takeoff presents the most difficult energy management task and therefore is chosen as an example maneuver to study the benefits of energy distribution control. A Zhu–Etkin[3] three-dimensional doublet sheet microburst model, which models both horizontal wind shear and downdraft, was chosen to simulate the wind-shear disturbances. A Monte Carlo simulation encompassing all the probable microburst encounters was conducted for two feedback controllers. A nonlinear controller using an inertial energy-based, constant gain, feedback structure is optimized based on 1) minimizing the maximum height-loss performance index (H-PI) and 2) minimizing an inertial energy distribution rate squared integral performance index (IED-PI). An acceleration guidance scheme defined by Miele et al.[14] is chosen as a baseline comparison for this study. The numerical results obtained are used to show 1) that IED-PI closely matches H-PI results, 2) the robustness of the constant gain feedback to various microburst environments, 3) the importance of distributing the inertial energy error equally between airplane kinetic and potential energies, 4) the minimization of height loss results in maintaining an approximately constant inertial speed, and 5) that inertial energy distribution error control provides superior trajectories compared to those of an acceleration guidance scheme for large microburst wind-shear encounters.

Problem Formulation

Energy Formulation

The total energy of the airplane is written as:

$$E = mgH_I + \tfrac{1}{2}mV_I^2 \tag{1}$$

where

mgH_I = total potential energy of the aircraft
$\frac{1}{2}mV_I^2$ = total kinetic energy of the aircraft

(The energy formulation presented here relates to a level flight condition and perturbations about the level flight condition. The formulation can be easily modified to represent other flight conditions.) The inertial energy distribution between potential and kinetic energies is defined as

$$\text{Energy distribution} = mgH_I - \tfrac{1}{2}mV_I^2 \tag{2}$$

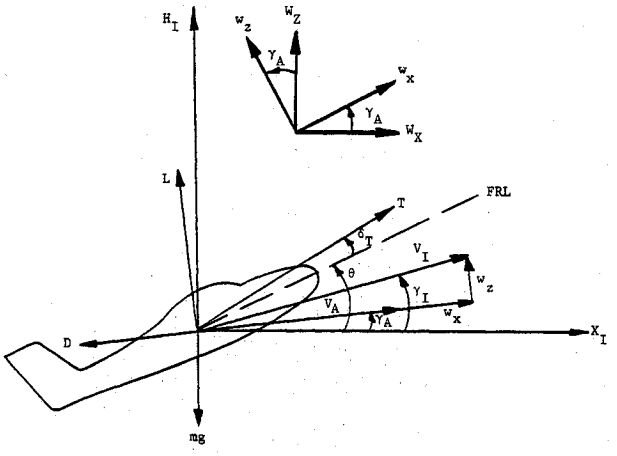

Fig. 2 Geometry of the longitudinal energy analysis.

The energy distribution does not immediately reveal itself as a good energy measure. Alternatively, an energy distribution error is defined. This error defines how any error in total energy is distributed between speed and height as

$$E_d = mg(H_I - H_{I0}) - \tfrac{1}{2}m(V_I^2 - V_{I0}^2) \tag{3}$$

This distribution error energy measure directly relates to energy equilbrium between the aircraft's potential and kinetic energy errors. The energy distribution rate is defined as

$$\dot{E}_d = mg\dot{H}_I - mV_I\dot{V}_I \tag{4}$$

Equation (1) defines the total energy of the aircraft with respect to inertial quantities, namely, inertial height and inertial speed. In the situation where wind and wind shear are present, the total energy can be written in terms of the total energy relative to the air mass and the wind-induced energy changes as

$$E = [mgH_A + \tfrac{1}{2}mV_A^2]_1 + [mgH_W + \tfrac{1}{2}(2V_A w_x + w_x^2 + w_z^2)]_2 \tag{5}$$

where (see Fig. 2)

$$H_A = \int V_A \sin\gamma_A \, dt$$
$$H_W = \int W_Z \, dt$$
$$w_x = W_X \cos\gamma_A + W_Z \sin\gamma_A$$
$$w_z = -W_X \sin\gamma_A + W_Z \cos\gamma_A$$
$$V_I^2 = (V_A + w_x)^2 + w_z^2$$
$[\ ]_1$ = total energy relative to air mass
$[\ ]_2$ = wind-induced energy changes

Differentiating this total energy with respect to time, we get the total energy rate of change as

$$\dot{E} = (mg\dot{H}_A + mV_A\dot{V}_A)_1 + (mg\dot{H}_W + m\dot{V}_A w_x + mV_A\dot{w}_x + mw_x\dot{w}_x + mw_z\dot{w}_z)_2 \tag{6}$$

where

$$(\ )_1 = \dot{E}_{\text{air mass}} \quad \text{and} \quad (\ )_2 = \dot{E}_{\text{wind}}$$

From the foregoing equations, we see that the wind-induced energy (referenced to the longitudinal wind axes) is caused by updrafts and downdrafts (w_z), horizontal wind (w_x) and horizontal wind shear ($\approx \dot{w}_x$), and vertical wind shear ($\approx \dot{w}_z$).

Inertial Energy Distribution Rate Performance Index

A performance index based on the minimization of the total inertial energy distribution error (IED-PI), during the microburst encounter, is defined as a Lagrange-type problem and is presented next.

$$J[u] = \int_{t_0}^{T} (\dot{E}_d)^2 \, dt \tag{7}$$

In the absence of any thrust inputs (i.e., the total energy change is only due to nonconservative energy transients and wind-induced energy losses), minimizing this performance index suggests an equal distribution of the available energy between potential energy and kinetic energy.

Another way to represent inertial energy distribution error rate is by rewriting it in terms of air mass relative parameters and wind energy loss parameters as[1]

$$\dot{E}_d = [mg\dot{H}_A - mV_A\dot{V}_A]_1 + [(mg\dot{H}_W - m\dot{V}_A w_x - mV_A\dot{w}_x - mw_x\dot{w}_x - mw_z\dot{w}_z)]_2 \tag{8}$$

where

$[\ ]_1$ = airmass relative distribution error rate

$[\ ]_2$ = energy loss rate associated with wind disturbances

The first term suggests that minimization of inertial energy distribution error minimizes the air mass relative distribution error. Air mass relative distribution error is the same as the inertial energy distribution error in the absence of wind disturbances. The second term shows that IED-PI also has knowledge of the energy lost to the wind, and thus minimizing IED-PI minimizes energy lost to the wind, which is highly desirable.

We can rewrite $\dot{E}_d$, after noting that $\dot{V}_I = \dot{H}_I(\dot{V}I/H_I)$, as

$$\dot{E}_d = mg\dot{H}_1\left(1 - \frac{V_I\dot{V}_I}{g\dot{H}_I}\right) = mg\dot{H}_I K(t) \tag{9}$$

where

$$K(t) = \left(1 - \frac{V_I\dot{V}_I}{g\dot{H}_I}\right) \tag{10}$$

The function $K(t)$ is viewed here as a time-varying penalty on $mg\dot{H}_I$ and its properties for a phugoid mode oscillation and wind-shear encounter are summarized as follows:

1) In a typical uncontrolled phugoid oscillation, either $\dot{H}_I < 0$ and $\dot{V}_I > 0$ (from the peak to the bottom) or $\dot{H}_I > 0$ and $\dot{V}_I < 0$ (from the bottom to the peak). This implies that $K(t)$ is always > 1.0 in a typical phugoid oscillation.

2) If no thrust is added to the system, in the headwind portion of the wind-shear encounter, if we assume negligible drag changes, $\dot{E} = 0$. This implies that $mg\dot{H}_I = -mV_I\dot{V}_I$ and $K(t) = 2.0$.

3) When shear is encountered, excessive losses in airspeed and phugoid mode excitation force $K(t) > 2.0$.

From the foregoing characteristics of $K(t)$, we can say that the IED-PI is equivalent to a perforamance index based on $\dot{H}_I$ with a varying penalty. The penalty increases with transients arising from both phugoid oscillations and nonconservative losses due to wind and wind shear. In other words,

$$J[u] = \int (\dot{E}_d)^2\,dt = \int (mg\dot{H}_I)^2K^2(t)\,dt \tag{11}$$

Miele et al.[5] showed that the optimal trajectories based on minimax gamma loss were considerably superior to constant angle-of-attack and constant pitch-angle trajectories in terms of avoidance of the ground. The close relationship between the minimax gamma (absolute flight-path angle) loss performance index analyzed in Ref. 5 and the IED-PI is shown next.

Assuming that $\sin\gamma \approx \gamma$, we have

$$J[u] = \int_{t_0}^{T} (\gamma_I - \gamma_{I0})^2K1^2(t)\,dt \tag{12}$$

where

$$\gamma_I = \arcsin\left(\frac{\dot{H}_I}{V_I}\right); \qquad K1(t) = mgV_IK(t)$$

Now, if damping due to drag terms is neglected, then the total energy is almost a constant ($\dot{E} = 0$). Because of losses in lift in the shear and entraining of the airplane in the downdraft, the potential energy decreases ($mg\dot{H}_I < 0$). This implies, from Eq. (1), that $mV_I\dot{V}_I > 0$, i.e., in the shear the inertial speed increases. This in turn implies that $K1^2(t)$ increases with increased height losses. With this observation in mind, Eq. (12) can be interpreted as being equivalent to the minimax gamma loss problem with $K1^2(t)$ as the penalty factor. $K1^2(t)$ increases nonlinearly whenever γ_I deviates from the reference value.

The preceding analysis revealed the height-loss minimization characteristics of the IED-PI through its various attributes regarding flight in a microburst wind-shear environment. The various contributing factors to the success of the IED-PI in minimizing height losses are summarized here.

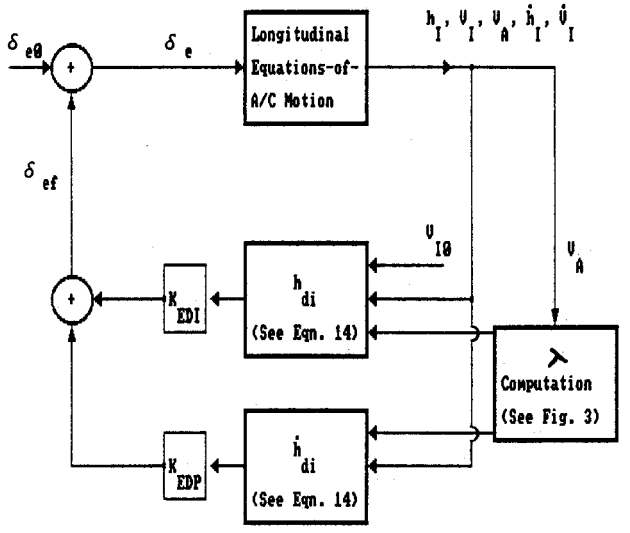

Fig. 3 Energy feedback control structure.

1) Rewriting IED-PI in terms of $mg\dot{H}_I$ and the penalty function $K(t)$ showed that minimizing IED-PI results in a well-damped phugoid mode.

2) The penalty function $K(t)$ remained close to 2.0 during the wind-shear encounter, and this showed a strong relationship between IED-PI and a height-loss minimization performance index, namely, minimax gamma loss.

3) Minimization of IED-PI minimizes the energy lost to the wind and also minimizes the energy distribution error between air mass relative potential energy and air mass relative kinetic energy.

Energy-Based Feedback Structure

Energy methods were used for analysis and feedback control of airplane flight in turbulence and wind by Jones.[7] Energy concepts were also developed separately by Lambregts[8] in his definition of the total energy control system (TECS) concept for an integrated flight control system. In Ref. 7, Jones showed that with fairly tight height control (feedback of height and height rate to elevator), although the resonance at phugoid frequency is largely removed, the spectral density of airspeed variations at the lowest frequencies is increased. This result is interpreted in terms of energy, as a channeling of energy error into speed. For instance, in the case of a microburst encounter, a tight height control (h and $\dot{h}$ feedback to elevator) will make the aircraft pitch up and reach stall conditions very quickly. Suppressing either the height error (height and height-rate error feedback to elevator) or speed error (V, $\dot{V}$ negative feedback to elevator) leads to increased losses in the other variable. The alternate strategy here is to control speed and height with equal importance. This strategy is achieved by feeding back the energy distribution error and its rate to the elevator.

The feedback structure used in this study is illustrated in Fig. 3. The feedback elevator perturbation control is computed based on the inertial energy distribution error between inertial height and inertial speed as

$$\delta_{ef} = K_{EDI}h_{di} + K_{EDP}\dot{h}_{di} \tag{13}$$

where

$$h_{di} = 2\lambda h_I - (2 - 2\lambda)\frac{V_I^2 - V_{I0}^2}{2g}$$

$$\dot{h}_{di} = 2\lambda\dot{h}_I - (2 - 2\lambda)\frac{V_I\dot{V}_I}{g} \tag{14}$$

The choice of using the specific inertial energy distribution error for elevator control, instead of the energy distribution based on airspeed (kinetic energy defined in terms of airspeed as used by Jones[7]), has the following advantages for a microburst encounter:

1) Better glide path control is achieved in the headwind portion of the microburst encounter by using specific inertial energy distribution error for elevator control. In contrast, if energy is distributed equally between airspeed and altitude, the aircraft will climb above the desired trajectory. This might not be desirable in landing approaches where glide slope tracking is crucial.

2) Accepting higher airspeed in headwind will help in trading this excess airspeed for altitude once the shear is encountered. Feeding back inertial energy distribution error to the elevator in a shear will equally distribute this stored energy between altitude and inertial speed. This strategy will make the aircraft pitch up in the high-shear portion, even though the airspeed might be dropping. This is a very desirable property of a controller for a microburst encounter.

Some of the drawbacks of feeding back the inertial energy distribution error to the elevator are airspeed regulation and insensitivity to performance reversal situations (operating in the back side of the drag curve). To overcome these drawbacks, an energy partition parameter λ (as defined by Jones[7]) is included in the definition of the inertial energy distribution parameters [see Eq. (14)]. When $\lambda = 1$, energy distribution fully favors height, and similarly when $\lambda = 0$, speed is the primary feedback variable. In general, λ can be chosen to have an optimal partition between height and speed. In this study, the choice of λ is based on the maximum allowable fluctuations in airspeed and a typical variation is graphed in Fig. 4. K_{1V} and K_{2V}, shown in Fig. 4, are optimized by augmenting the original performance index with penalty functions.

During performance reversal situations, λ linearly varies until it becomes zero, suggesting no height control, and an elevator is used to control airspeed. When airspeed builds up above normal allowable upper limit, λ reaches 1.0, the distribution error is biased toward height, and all the excess kinetic energy is converted into potential energy.

Aircraft System Description

In this study, a body-fixed-axes[17] system is used to define the longitudinal aircraft dynamic equations. The aircraft used for the simulation study is a Boeing B-727 aircraft powered by three JT8D-17 turbofan engines. The kinematic and dynamic body-axis equations of motion (augmented with the linearized short-period dynamics equation) are

$$\begin{aligned}
\dot{X}_I &= U\cos\theta + W\sin\theta \\
\dot{H}_I &= U\sin\theta - W\cos\theta \\
m\dot{U} &= (T\cos\delta)\delta_t + L\sin\alpha - D\cos\alpha \\
&\quad - mg\sin\theta - mWq \\
m\dot{W} &= (-T\sin\delta)\delta_t - L\cos\alpha + D\sin\alpha \\
&\quad + mg\cos\theta - mUq + Z_e\delta_e \\
\dot{q} &= M_u u + M_w w + M_q q + M_t\delta_t \\
&\quad - (M_u\cos\theta_0 + M_w\sin\theta_0)W_X \\
&\quad - (M_u\sin\theta_0 - M_w\cos\theta_0)W_Z + M_e\delta_e \\
\dot{\theta} &= q
\end{aligned} \tag{15}$$

These equations are supplemented by the functional relations

$$T = T(V_A); \quad L = L(V_A, \alpha); \quad D = D(V_A, \alpha)$$

$$W_X = W_X(X_I, H_I); \quad W_Z = W_Z(X_I, H_I)$$

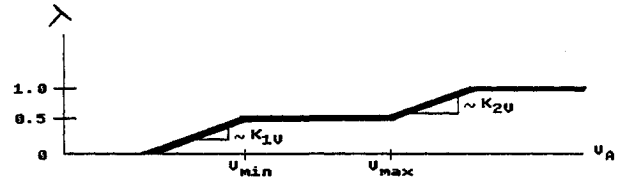

Fig. 4 Variation of λ with airspeed.

and the analytical relations

$$V_I = \sqrt{U^2 + W^2}$$

$$V_A = \sqrt{(U - w_x)^2 + (W - w_z)^2}$$

$$w_x = W_X\cos\gamma_A - W_Z\sin\gamma_A$$

$$w_z = W_X\sin\gamma_A + W_Z\cos\gamma_A$$

$$\alpha = \arctan\left(\frac{W - w_z}{U - w_x}\right)$$

$$\gamma_A = \arctan\left(\frac{\dot{H}_I - W_Z}{\dot{X}_I - W_X}\right)$$

The system just presented involves six state variables (X_1, H_1, U, W, q, θ) and two control variables (δ_e, δ_t). On the basis of the assumption that the power setting is at the maximum level during takeoff, the number of controls reduces to one (elevator control only). Nonlinear limits on the angle of attack and elevator deflection are also imposed.

Genetic Algorithm Controller Gain Optimization

A genetic algorithm optimization technique is utilized to determine the optimum feedback controller gains based on the chosen performance index. The genetic algorithm's mechanism models the process of natural genetics, combining a Darwinian survival of the fittest with randomized yet structured information exchange among a population of artificial chromosome.[9,16] Each feedback gain of the controller structure is mapped to a binary string representation. To get a starting population, a number of such binary strings are generated randomly. For each successive generation, the strings are reproduced based on their performance index (fitness rule) with information exchange (crossover) between these strings occurring with a preselected probability of crossover. To improve the global nature of the search, the mutation operation (altering a single bit at random) is used with a preselected probability of mutation.

Genetic algorithms are different from the normal search methods encountered in engineering optimization. Genetic algorithms require the natural parameter set of the optimization problem to be coded on a finite-length string. For example, in the optimization problem presented here, the three gain controller is discretized by mapping from a smallest possible gain set $K_{\min}$ to a largest possible gain set $K_{\max}$, using a 10-bit binary unsigned integer for each of the $K_j (j = 1, 2, 3)$. In this coding, a string code 0000000000 maps to $K_{\min}$ and 1111111111 maps to $K_{\max}$ with a linear mapping in between. Now the three 10-bit gain sets are chained together to form a 30-bit string representing a particular controller design. A single 30-bit string represents one of the 2^{30} alternative solutions. Genetic algorithms work iteration by iteration, generating and testing a population of strings. This population-by-population approach is similar to a natural population of biological organisms in which each generation successfully evolves into the next generation by being born and raised until it is ready to reproduce.

The genetic algorithm was originally developed by Holland[10] and has been applied to many parameter optimization problems by Goldberg and others,[11,12] emphasizing the al-

gorithm's paramount ability to identify a global minimum from local minima. When a large set of objective functions of unknown character is to be evaluated, the genetic algorithm offers an easy-to-implement approach that is insensitive to the character of the objective function.

Performance of the wind-shear control system for the current set of feedback gains is directly measured by a particular objective function. Each new-generation set of gains is reproduced by applying the fitness rule, crossover, and mutation to the current generation gain set, and the search is terminated when the whole population converges to the optimum.

Monte Carlo Simulation

A Monte Carlo simulation of an airplane flight in wind shear over all probable sizes and strengths of microburst wind-shear disturbances was conducted to fulfill the following objectives:

1) Show that the constant-gain inertial energy distribution feedback controller based on IED-PI is robust over all probable wind-shear encounters.

2) Show that the height-loss minimization characteristics of the IED-PI are equivalent to the minimax height loss PI (H-PI).

To achieve the aforementioned objectives, first, feedback gains are optimized based on minimization of the IED-PI for a nominal microburst encounter for the takeoff phase of an airplane flight. These constant feedback gains are then used to control an airplane microburst encounter over all probable microburst sizes and strengths. Second, controllers based on H-PI are optimized for each microburst encounter in the sample set of all probable microburst sizes and strengths. In all, 800 takeoff simulations in the presence of random microburst environments were simulated for the IED-PI-based controller and were compared with the H-PI trajectory data. The results are used to show the robustness of the constant gain controller based on IED-PI and its excellent height-loss minimization characteristics.

Microburst Strength and Size Distributions

In this study, the microburst strength is considered to be directly related to the maximum horizontal wind-shear velocity differential associated with the microburst wind profiles. The Zhu–Etkin model[3] is used to define the microburst structure. The Zhu–Etkin microburst model strength and its number of doublet sheets were chosen to provide the following: 1) The desired maximum horizontal wind differential. 2) The desired ratio of maximum horizontal wind differential to maximum vertical wind (chosen to be 2.0 for this study).

A Rayleigh density function was utilized to fit the statistical data derived from the JAWS weather studies presented in Ref. 13 for ΔW_X with the following parameters.

Rayleigh density function:

$$f(x) = \frac{x}{\rho^2}\exp\left(\frac{-x^2}{2\rho^2}\right)$$

$$x \geq 0$$

$$x = \Delta W_X - 20 \text{ ft/s}$$

$$\rho = 50 \text{ ft/s}$$

The center of the microburst vortex sheet is fixed at 3300 ft above the ground and a uniform density function was chosen for the microburst size. In terms of the Zhu–Etkin model, the size was defined as a uniform density function with 6000 ft $\leq D \leq$ 12,000 ft, where D is the diameter of the doublet sheet.

Takeoff Maneuver Definition

The takeoff maneuver simulated is defined in a vertical plane that passes through the runway centerline. It is assumed that the aircraft is airborne and is initialized on a climb path. In takeoff, it is also assumed that the power is set at the maximum value, and that elevator is the only control available. The takeoff airspeed is assumed to be trimmed to the wind speed at the time of the simulation initialization. The constant climb starts at a distance of $X_I = 0$ ft, and the climb ends at a distance of $X_I = 20{,}000$ ft.

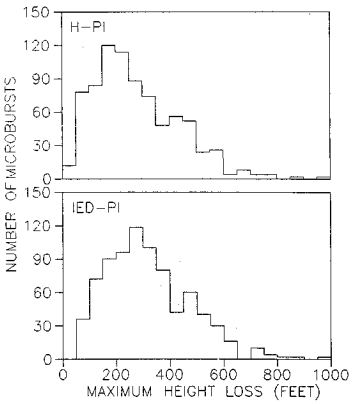

Fig. 5 Frequency distribution of maximum height loss for IED-PI and H-PI.

Table 1 Statistics of the simulation results

Aircraft variable	Mean		Standard deviation	
	IED-PI	H-PI	IED-PI	H-PI
Maximum height loss	319	279	156	159
Minimum airspeed	235	229	15.3	15.0
Maximum airspeed	312	317	12.8	14.5
Minimum inertial speed	260	255	8.7	9.8
Maximum inertial speed	278	278	1.9	0.9
Minimum inertial energy distribution error	−288	−188	129	135
Maximum inertial energy distribution error	151	45	49	22

Monte Carlo Takeoff Simulation Results

Eight hundred takeoff simulations, 400 each for a IED-PI controller and H-PI controller, under the presence of wind shear were conducted with random microburst strength and size as determined by the microburst statistical models defined earlier. The initial and final conditions, reference vectors, and nonlinear limits defined in the Appendix were used for each run. The results obtained are presented as the frequency distribution of maximum deviations (from the desired values) of altitude, inertial speed, and inertial specific energy distribution. Table 1 presents the summary statistics of the simulation results.

Height Loss

Figure 5 presents the frequency distribution of maximum height losses from the desired trajectory for IED-PI and H-PI. These results show the good height-loss minimization characteristics of IED-PI and its equivalent performance to that of H-PI (see Table 1). The lower mean and standard deviations for IED-PI reflect better height control. Good correlation between IED-PI and H-PI performances in terms of equal standard deviations suggest the insensitivity of the controller gain set to varying microburst profiles.

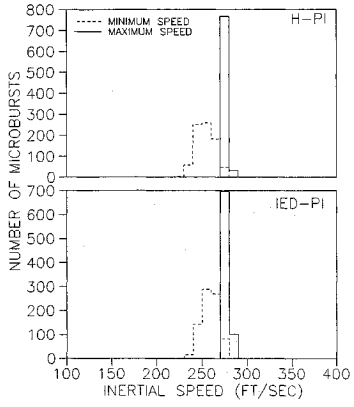

Fig. 6 Frequency distribution of inertial speed deviations for IED-PI and H-PI.

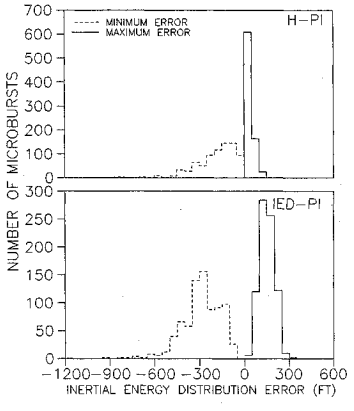

Fig. 7 Frequency distribution of inertial specific energy distribution error for IED-PI and H-PI.

Inertial Speed

Figure 6 presents the distribution for inertial speed deviations for IED-PI and H-PI, respectively. This suggests that to minimize height losses, under the absence of any additional energy through throttle inputs, it is important to maintain approximatley constant inertial speeds. This result is interpreted in two ways: 1) Constant inertial speed directly implies a well-damped phugoid mode. 2) Maintaining constant inertial speed in the headwind implies accepting the increase in airspeed due to headwind. This stored air mass relative kinetic energy is traded for potential energy once shear is penetrated. Maintaining constant inertial speed in the tailwind shear implies accepting losses in airspeed and converting all the excess air mass relative kinetic energy into potential energy, in order to minimize height losses.

Inertial Energy Distribution Error

As mentioned earlier, to minimize height losses it is important to distribute the available energy. Figure 7 emphasizes this importance via the low mean and standard deviations of the inertial specific energy distribution error for IED-PI and H-PI. Statistics of H-PI show that to minimize maximum height losses, it is essential to distribute energy equally between height and inertial speed.

Comparison of IED Control with an Acceleration Guidance Scheme

In the past few years, many optimal and optimal guidance schemes for flight in wind shear have been derived and tested.[4–6,14,15] Of these studies, Miele et al.[4,5,14,15] present some of the most significant contributions in terms of providing an understanding of the optimal control trajectories and equivalent guidance strategies for wind-shear encounters. In Refs. 14 and 15, Miele et al. present two relatively superior guidance strategies, namely, acceleration guidance and gamma guidance, for flight in wind shear.

In this section, the IED controller is compared with the acceleration guidance scheme (AC-GS)[14] (Miele et al. show in Ref 15 that gamma guidance and acceleration guidance exhibit similar performances). This comparison is conducted to emphasize the superior wind-shear control capability of the IED-PI controller. The acceleration guidance law is obtained by taking note of the fact that the relative acceleration $(\dot{V}_A/g)$ is approximately proportional to a shear/downdraft factor F defined by the equation

$$F=\left(\frac{\dot{W}_X}{g}\right)\cos\gamma_A+\left(\frac{\dot{W}_Z}{g}\right)\sin\gamma_A-\frac{W_Z}{V_A} \tag{16}$$

Based on this fact, an analytical form is derived from the equations of motion (for a detailed derivation, see Ref. 14).

$$\left(\frac{T}{W}\right)\cos(\alpha+\delta)-\frac{D}{W}-\sin\gamma_A-G=0 \tag{17}$$

$$G=(1-C)\left[\left(\frac{\dot{W}_X}{g}\right)\cos\gamma_A+\left(\frac{\dot{W}_Z}{g}\right)\sin\gamma_A\right]+C\left(\frac{W_Z}{V_A}\right) \tag{18}$$

where C is a dimensionless constant chosen[14] to be 0.5. The foregoing equation is used to derive an explicit guidance law for α in the form

$$\alpha=f(V_A, W_X, W_Z, \gamma_A) \tag{19}$$

The explicit guidance scheme just presented was implemented for the system described earlier (without the short period augmentation). Two Zhu–Etkin microburst wind profiles were used to make a comparison in the trajectories of the resulting flight in wind shear for the AC-GS and IED-PI controllers. A mean microburst wind-shear profile, ZE-1, derived from the distribution presented earlier and a severe microburst wind shear, ZE-2, that reflects a 2-sigma deviation from the mean are used as the two Zhu–Etkin example microburst wind-shear profiles. Figures 8–11 show the wind

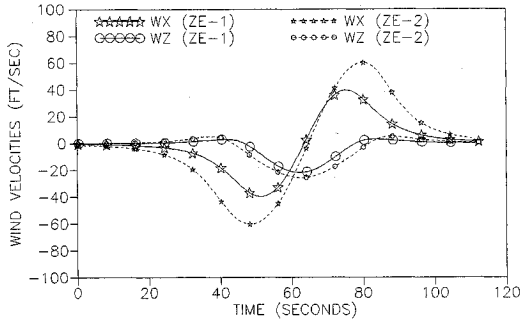

Fig. 8 Microburst wind profiles for ZE-1 and ZE-2.

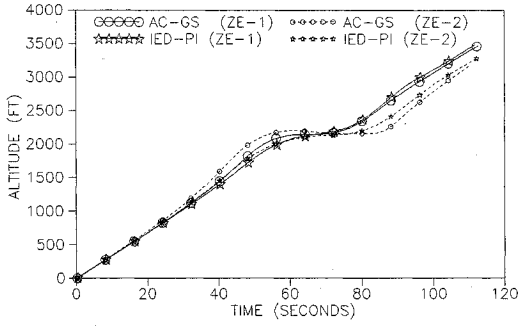

Fig. 9 Height response for microbursts ZE-1 and ZE-2.

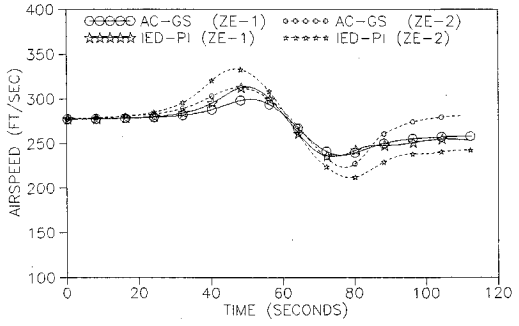

Fig. 10 Airspeed response for microbursts ZE-1 and ZE-2.

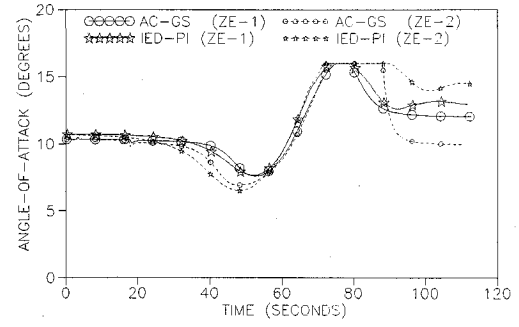

Fig. 11 Angle-of-attack response for microbursts ZE-1 and ZE-2.

velocities, height, airspeed, and angle-of-attack trajectories, respectively, for ZE-1 and for ZE-2. Based on these figures, the following comments are made.

1) The altitude responses of the IED-PI controller for ZE-1 and ZE-2 show the benefits of minimizing inertial distribution error. The aircraft, after encountering the shear, levels out to trade potential energy for inertial kinetic energy. At the end of the shear, the airplane continues on its climb path. Maintaining a level flight through a severe shear is important for two reasons: a) Continuing to climb in high wind shears will result in excessive losses in airspeed. This will result in an early stall situation from which recovery might be impossible. b) In a typical microburst environment, the vertical wind component increases with altitude. This makes it more essential to level out at a lower altitude until the end of the shear.

2) Both IED-PI and AC-GS show similar performances for ZE-1, but for ZE-2, the IED-PI controller shows a better monotonic altitude response and lower height loss; and IED-PI permits more airspeed increases in the headwind and thus controls the trajectory better, in both the headwind and shear.

3) Both angle-of-attack trajectories exhibit an initial decrease followed by a sustained increase to the stall limit.

Conclusions

The principle of inertial energy distribution error control for optimal wind-shear penetration was developed theoretically, and a controller based on this principle was experimentally tested for a takeoff flight condition to demonstrate its application capabilities. Results of the experimental study demonstrated the excellent height-minimization characteristics of the controller based on the inertial energy distribution error rate performance index. Major results obtained in this study are summarized as follows:

1) Relationships between the inertial energy distribution error rate performance index and minimax gamma loss performance index were established and used to substantiate the use of the inertial energy distribution performance index (IED-PI) for control system implementation.

2) Concepts of controlling inertial energy distribution error to achieve optimal wind shear guidance, by feeding back inertial energy quantities to an elevator, in a manner similar to the airspeed-based energy ideas suggested by Jones, were introduced.

3) Monte Carlo simulation of the takeoff flight condition was conducted to demonstrate the robustness of the IED controller to varying microburst environments. Results from the Monte Carlo simulation demonstrated the equivalent performance characteristics of H-PI and IED-PI. The results also substantiated two important concepts: a) To minimize height losses, it is important to distribute inertial energy error equally between potential energy and inertial kinetic energy. b) Minimization of height loss results in maintaining an approximately constant inertial speed (i.e., ground speed).

4) Both IED-PI and AC-GS showed similar performances for a medium microburst encounter. For a large microburst encounter, the IED controller exhibited superior performance.

Appendix: Data for the Monte Carlo Simulation

The aircraft used for the simulation study is a Boeing B-727 aircraft powered by three JT8D-17 turbofan engines.

Initial Conditions for the Takeoff Maneuver

$$X_I = 0 \text{ ft}$$
$$H_I = 100 \text{ ft}$$
$$V_A = 276.94 \text{ ft/s}$$
$$U = 273.71 \text{ ft/s}$$
$$W = 42.15 \text{ ft/s}$$
$$\alpha = 10.75 \text{ deg}$$
$$\theta = 15.75 \text{ deg}$$
$$\gamma = 7.0 \text{ deg}$$
$$\delta_t = 0.99$$
$$\delta_e = 0.386 \text{ rad}$$

Final Conditions for the Maneuver

$$X_I = 20{,}000 \text{ ft}$$

Controller Design Parameters

$$V_{\min} = 225 \text{ ft/s}$$

$$V_{\max} = 325 \text{ ft/s}$$

References

[1]Bailey, J. E., and Krishnakumar, K. S., "Total Energy Control Concepts Applied to Flight in Wind Shear," AIAA Paper 87-2344, 1987.

[2]Fujita, T. T., DFW *Microburst on August 2, 1985*, Satellite and Mesometeorology Research Project, University of Chicago, Chicago, IL, 1986.

[3]Zhu, S., and Etkin, B., "Fluid-Dynamic Model of a Downburst," Univ. of Toronto, Toronto, Canada, UTIAS Rept. 271, CNISSM 0082-5255, 1983.

[4]Miele, A., Wang, T., Tzeng, C. Y., and Melvin, W. W., "Optimization and Guidance of Abort Landing Trajectories in a Wind Shear," AIAA Paper 87-2341, 1987.

[5]Miele, A., Wang, T., and Melvin, W. W., "Optimal Flight Trajectories in the Presence of Wind Shear; Part 1, Take-off," AIAA Paper 85-1843, 1985.

[6]Psiaki, M. L., and Stengel, R. F., "Analysis of Aircraft Control Strategies for Microburst Encounter," *Journal of Guidance, Control, and Dynamics*, Vol. 8, No. 5, 1985, pp. 553–559.

[7]Jones, J. G., "Application of Energy Management Concepts to Flight-Path Control in Turbulence," AGARD-CP-140, 1973.

[8]Lambregts, A. A., "Vertical Flight Path and Speed Control Autopilot Design Using Total Energy Principles," AIAA Paper 83-2239, 1983.

[9]Goldberg, D. E., *Genetic Algorithm in Search, Optimization, and Machine Learning*, Addison Wesley, Reading, MA, 1988.

[10]Holland, J., *Adaptation in Natural and Artificial Systems*, University of Michigan Press, Ann Arbor, MI, 1975.

[11]Goldberg, D. E., and Samtani, M. P., "Engineering Optimization

via Genetic Algorithm," *Proceedings of the 9th Conference on Electronics Computation*, American Society of Civil Engineers, Birmingham, AL, 1986.

[12]Goldberg, D. E., "Computer-Aided Gas Pipeline Operation Using Genetic Algorithms and Rule Learning," Ph.D. dissertation, Dept. of Civil Engineering, Univ. of Michigan, Ann Arbor, MI, 1983.

[13]McCarthy, J., Roberts, R., and Schreiber, W., *JAWS Data Collection, Analysis Highlights, and Microburst Statistics*, Preprints, 21st Radar Meteorology Conference, Edmonton, Canada, pp. 596–601.

[14]Miele, A., Wang, T., and Melvin, W. W., "Optimization and Acceleration Guidance of Flight Trajectories in a Wind Shear," *Journal of Guidance, Control, and Dynamics*, Vol. 10, No. 4, 1987, pp. 368–377.

[15]Miele, A., Wang, T., and Melvin, W. W., and Bowles, R. L., "Gamma Guidance Schemes for Flight in a Wind Shear," *Journal of Guidance, Control, and Dynamics*, Vol. 11, No. 4, 1988, pp. 320–327.

[16]Goldberg, D. E., Course notes and personal conversation, Dept. of Engineering Mechanics, Univ. of Alabama, Tuscaloose, AL, 1987.

[17]Etkin, B., *Dynamics of Atmospheric Flight*, Wiley, Toronto, 1972.

Recommended Reading from the AIAA Progress in Astronautics and Aeronautics Series . . . AIAA

Monitoring Earth's Ocean, Land and Atmosphere from Space: Sensors, Systems, and Applications

Abraham Schnapf, editor

This comprehensive survey presents previously unpublished material on past, present, and future remote-sensing projects throughout the world. Chapters examine technical and other aspects of seminal satellite projects, such as Tiros/NOAA, NIMBUS, DMS, LANDSAT, Seasat, TOPEX, and GEOSAT, and remote-sensing programs from other countries. The book offers analysis of future NOAA requirements, spaceborne active laser sensors, and multidisciplinary Earth observation from space platforms.

***TO ORDER:* Write, Phone, or FAX:** AIAA c/o TASCO, 9 Jay Gould Ct., P.O. Box 753, Waldorf, MD 20604 Phone (301) 645-5643, Dept. 415 ■ FAX (301) 843-0159

Sales Tax: CA residents, 7%; DC, 6%. For shipping and handling add $4.75 for 1–4 books (call for rates for higher quanties). Orders under $50.00 must be prepaid. Foreign orders must be prepaid. Please allow 4 weeks for delivery. Prices are subject to change without notice. Returns will be accepted within 15 days.

1985 830 pp., illus. Hardback
ISBN 0-915928-98-1
AIAA Members $59.95
Nonmembers $99.95
Order Number V-97